Hindawi
Journal of Nanomaterials
Volume 2023, Article ID 7685458, 7 pages
https://doi.org/10.1155/2023/7685458

Research Article

A Laminated Beam Model for the Effective Tensile and Bending Elastic Moduli of Nanowires

Quan Yuan and Qian He

School of Architectural and Civil Engineering, Xihua University, Hongguang Town, Chengdu 610039, China

Correspondence should be addressed to Quan Yuan; yuanqxh@163.com

Received 16 July 2022; Revised 28 December 2022; Accepted 28 January 2023; Published 21 February 2023

Academic Editor: Zafar Iqbal

Surface elasticity has a strong influence on the size-dependent mechanical properties of nanowires (NWs). In this work, a laminated beam model is used to predict the effective tensile and bending moduli of a NW. The surface layer is assumed to have a definite thickness and different elastic moduli from the bulk layer. The effective moduli of the NW are expressed as a function of surface thickness and surface constant. The theoretical predictions for stiffening and softening effects are in good agreement with experimental results. High surface elasticity increases the bending modulus more than the tensile modulus. Low surface elasticity decreases the bending modulus more than the tensile modulus. Surface thickness has a considerable influence on the effective modulus of NW and amplifies stiffening and softening effects.

1. Introduction

The role of the surface and the modeling of the surface effect are two important problems encountered in the theoretical prediction of the size-dependent behavior of nanowires (NWs) [1–9]. Eringen's nonlocal theory [10–12] and Gurtin and Murdoch's surface elasticity theory [4, 13, 14] are two widely used approaches for studying the small-scale effect on the tensile and flexural properties of NWs. Within these two theoretical frameworks of continuum mechanics, the surface is assumed to be zero and modeled as a two-dimensional membrane ideally adhering to the bulk of NWs. Miller and Shenoy [15] employed only one surface elastic constant to describe surface elasticity. The surface parameter measured via direct atomistic simulation can be positive or negative. Hence, surface stress can be positive or negative. Their continuum mechanics model shows that the effective tensile and bending elastic moduli of nanostructures can be larger or smaller than the bulk elastic modulus. Several recent works have extended Shenoy's formula to study the vibration and buckling of NWs [2, 3, 16, 17]. However, the exposition on the flexural resistance of surfaces in Gurtin–Murdoch surface elasticity theory and Shenoy's formula is unclear. In addition, surface thickness is equivocally defined as the ratio of the surface constant to the bulk modulus. In the case of a negative surface constant, surface thickness may be unrealistically negative. Steigmann and Ogden [18] established a curvature-dependent surface elasticity model to rectify the aforementioned deficiency. Chhapadia et al. [19] later generalized this work to predict the stiffening effect (positive surface elastic constants increase flexural rigidity more than tensile stiffness) and softening effect (negative surface elastic constants decrease flexural rigidity more than tensile stiffness) of the surfaces of NWs. Two elastic constants are introduced to describe surface tension and surface bending. The two parameters can also be negative. They provide a physically intuitive formula for defining the thicknesses of the surfaces of NWs. The defined thickness is finite and positive no matter the sign of the surface elastic constants. This situation indicates that the surface can be modeled as a shell layer with a constant thickness, and NW is considered to be a laminate of composite materials.

In principle, if surface thickness and elastic modulus are selected appropriately, the core–shell model can be used to investigate the size dependence of NWs. The stiffening effect for circular ZnO NWs has been successfully predicted by using the core–shell composite model [20, 21]. Yao et al. [22] proposed a modified core–shell model to describe the inhomogeneity of the surface shell. They assumed that the elastic

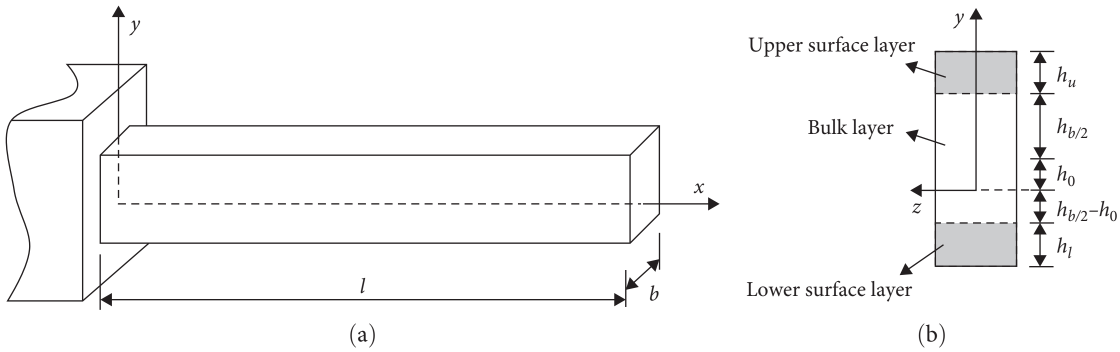

FIGURE 1: (a) The geometry of nanowire; (b) the cross-section of nanowire.

modulus of the surface shell exponentially varies along the thickness direction of NWs. In their work, the thickness of the surface shell is treated as an adjustable parameter to characterize the stiffening and softening effects. However, Shenoy's formula [15] and Chhapadia's model [19] indicate that the thickness of the surface shell is constant. Improving the use of the core–shell model is the main motivation of this work. In this study, we employ a laminated beam model with a finite surface thickness to study the effective tensile and bending elastic moduli of a rectangular NW. The results of our model are compared with those of Shenoy's formula and Chhapadia's predictive model. Our formula, which has only two surface parameters, namely, thickness and elastic modulus, provides a good prediction for the stiffening and softening effects.

2. Model Analysis

As shown in Figure 1, we consider a rectangular nanowire to be a laminated beam with length $l (0 \le x \le l)$, thickness h, and width b. This sandwich beam is generally composed of two surface layers and a bulk core, as shown in Figure 1(b). The thicknesses of the upper, lower, and middle layers are denoted by h_u, h_l, and h_b, respectively. The bulk elastic modulus E_b of the middle layer is assumed to be constant, whereas surface elasticity and residual surface stress are assumed to vary in the thickness direction in accordance with exponential law and a special power law distribution [22, 23]. This condition gives us the following expressions: for the upper surface layer,

$$E_{su}(y) = E_b e^{\left(\frac{y - \frac{h_b}{2} - h_0}{h_u}\right)m}, \qquad \tau_{su} = \tau_u \left(\frac{y - \frac{h_b}{2} - h_0}{h_u}\right)^{\lambda}, \tag{1}$$

for the lower surface layer,

$$E_{sl}(y) = E_b e^{\left(\frac{h_0 - \frac{h_b}{2} - y}{h_l}\right)n}, \qquad \tau_{sl} = \tau_l \left(\frac{h_0 - \frac{h_b}{2} - y}{h_l}\right)^{\kappa}. \tag{2}$$

In above equations, τ represents the residual surface stress, and h_0 denotes the height of the neutral axis from the middle line of the bulk layer. Note that the four parameters m, n, λ, and κ describe the variation profile of material properties across surface layer thickness. We first consider the effective elastic modulus of the axially forced sandwich beam. The upper, middle, and lower layers are loaded in the x-direction with the same strain ε. In accordance with the formulation of the continuum of composite material, the force transmitted across the cross-section per unit width is given by the following equation:

$$N = \int_{h_0 - \frac{h_b}{2}}^{h_0 + \frac{h_b}{2}} E_b \varepsilon dy + \int_{h_0 + \frac{h_b}{2}}^{h_0 + \frac{h_b}{2} + h_u} (E_{su}\varepsilon + \tau_{su}) dy + \int_{h_0 - \frac{h_b}{2} - h_l}^{h_0 - \frac{h_b}{2}} (E_{sl}\varepsilon + \tau_{sl}) dy. \tag{3}$$

The internal force N equals the product of the applied stress σ and h ($N = \sigma h$). By substituting Equations (1) and (2) in Equation (3), the applied stress is expressed as follows:

$$\sigma = \frac{E_b \varepsilon}{h}\left[h_b + \frac{h_u(e^m - 1)}{m} + \frac{h_l(e^n - 1)}{n}\right] + \frac{1}{h}\left[\frac{\tau_u h_u}{(\lambda + 1)} + \frac{\tau_l h_l}{(\kappa + 1)}\right]. \tag{4}$$

The effective tensile elastic modulus is defined as $E_{et} = d\sigma / d\varepsilon$ under axial deformation. From Equation (4), the normalized effective elastic modulus is obtained as follows:

$$\frac{E_{et}}{E_b} = 1 + \frac{h_u(e^m - m - 1)}{hm} + \frac{h_l(e^n - n - 1)}{hn}. \tag{5}$$

As inferred from the expression of the effective tensile elastic modulus, the residual surface stress has no influence on E_{et}. The four surface constants may be computed by using atomistic simulation or measured through experiments. The influence of the signs of m and n on the size-dependency of NWs is presented in the next section.

We then consider the bending deformation of the sandwich beam. We use the laminated beam model to explain the flexural resistance of the surface layer to predict the effective bending elastic modulus of the NW. On the basis of the plane hypothesis of bending deformation, the axial strain of the beam is:

$$\varepsilon_x = -w''y, \tag{6}$$

where w'' is the bending curvature. The negative sign in the above equation implies compression in the region over the neutral axis. The stress–strain relation of the bulk is:

$$\sigma_x = E_b\varepsilon_x. \tag{7}$$

The stresses of the surface layers can be given as follows:

$$\sigma_s = \tau_s + E_s\varepsilon_x. \tag{8}$$

Note that $\sigma_s = 0$ when $\varepsilon_x = 0$. The residual surface stress is considered only when the NW is subjected to load. First, the surface stress and stress in the bulk balance the force, and integration over the cross-sectional area yields:

$$\int_{\Omega b}\sigma_x dA + \int_{\Omega s}\sigma_s dA = 0. \tag{9}$$

By substituting Equations (6–8) into Equation (9), we obtain the following equation:

$$\begin{aligned}&-E_b w''\left[h_b h_0 + \frac{e^m-1}{m}h_u\left(h_0+\frac{h_b}{2}\right) + \frac{e^m(m-1)+1}{m^2}h_u^2\right.\\&\left.-\frac{e^n-1}{n}h_l\left(\frac{h_b}{2}-h_0\right) - \frac{e^n(n-1)+1}{n^2}h_l^2\right]\\&+\frac{\tau_u h_u}{\lambda+1}+\frac{\tau_l h_l}{\kappa+1}=0.\end{aligned} \tag{10}$$

As found from the above equation, the height of neutral axis $h_0 \neq 0$ if the upper and lower surface layers have different thicknesses or surface elasticities. Equation (10) also implies that the change in the height of the neutral axis with the position of the cross-section can be attributed to the bending curvature and the residual surface stress. h_0 is a function of the curvature w''. Second, the surface stress and stress in the bulk balance the applied moment M, and integration over the surface and bulk layer yields:

$$-\int_{\Omega b}\sigma_x y dA - \int_{\Omega s}\sigma_s y dA = M. \tag{11}$$

By substituting Equations (6–8) into Equation (11), we obtain the following equation:

$$\begin{aligned}&E_b b w''\left\{\left(\frac{1}{12}h_b^3 + h_b h_0^2\right) + \frac{e^m-1}{m}h_u\left(h_0+\frac{h_b}{2}\right)^2 + \frac{2[e^m(m-1)+1]}{m^2}h_u^2\left(h_0+\frac{h_b}{2}\right)\right.\\&+\frac{e^m(m^2-2m+2)-2}{m^3}h_u^3 + \frac{e^n-1}{n}h_l\left(h_0-\frac{h_b}{2}\right)^2 + \frac{2[e^n(1-n)-1]}{n^2}h_l^2\left(h_0-\frac{h_b}{2}\right)\\&\left.+\frac{e^n(n^2-2n+2)-2}{n^3}h_l^3\right\} - \frac{\tau_u b h_u}{\lambda+1}\left(\frac{h_b}{2}+h_0+h_u-\frac{h_u}{\lambda+2}\right) + \frac{\tau_l b h_l}{\kappa+1}\left(\frac{h_b}{2}-h_0+h_l-\frac{h_l}{\kappa+2}\right) = M.\end{aligned} \tag{12}$$

As found from the above equation, the nonlinear differential equation for the deflection of a laminated beam is different from that of an Euler–Bernoulli beam (h_0 varies with x). If we let $m \longrightarrow 0$, $n \longrightarrow 0$, and $\tau_u = \tau_l = 0$, Equation (12) is simplified into the classical model. For the sake of simplicity, we study a symmetrical laminated beam. Letting $h_u = h_l = h_s$, $\lambda = \kappa$, $m = n$, only two constants remain for the characterization of surface elasticity. Equations (10) and (12) can also be expressed by the following equation:

$$\begin{aligned}&-E_b w'' h_0\left[h_b + \frac{2(e^m-1)}{m}h_s\right] + \frac{(\tau_u+\tau_l)h_s}{\lambda+1} = 0,\\&E_b b w''\left\{\left(\frac{1}{12}h_b^3 + h_b h_0^2\right) + \frac{2(e^m-1)}{m}h_s\left(h_0^2+\frac{h_b^2}{4}\right)\right.\\&\left.+\frac{2[e^m(m-1)+1]}{m^2}h_s^2 h_b + \frac{2[e^m(m^2-2m+2)-2]}{m^3}h_s^3\right\}\\&-\frac{\tau_u-\tau_l}{\lambda+1}bh_s\left(\frac{h_b}{2}+\frac{\lambda+1}{\lambda+2}h_s\right) - \frac{\tau_u+\tau_l}{\lambda+1}bh_s h_0 = M.\end{aligned} \tag{13}$$

As noted in Equation (13), the self-balancing residual surface stress has no influence on deformation when the bending curvature is zero. Then, from Equation (13), the height of the neutral axis can be written as follows:

$$h_0 = \frac{(\tau_u+\tau_l)h_s R}{E_b w''(\lambda+1)\left[h_b + \frac{2(e^m-1)}{m}h_s\right]}. \tag{14}$$

As found from the above equation, $h_0 = 0$ when $\tau_u = \tau_l = 0$, that is, the neutral axis coincides with the centroidal axis on the section. However, positive residual surface stress (surface tension) causes the neutral axis to drop, and negative residual surface stress (surface compression) causes the neutral axis to rise. By substituting Equation (14) into Equation (13), we obtain the second-order differential equation:

$$w'' = \frac{M+a_2}{a_1}, \tag{15}$$

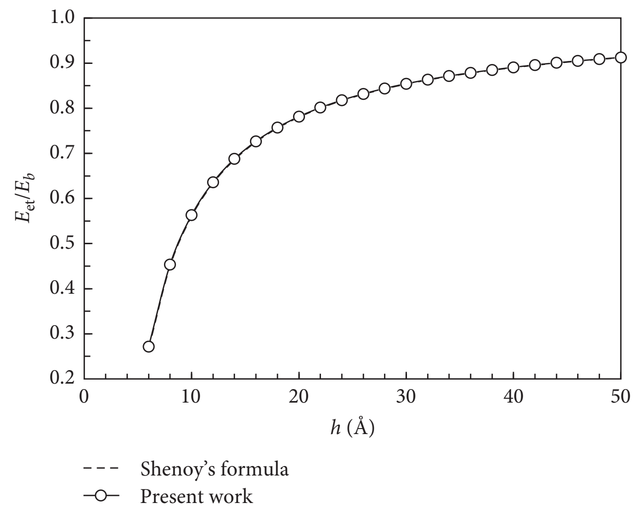

FIGURE 2: Effective tensile elastic modulus of Si nanowires.

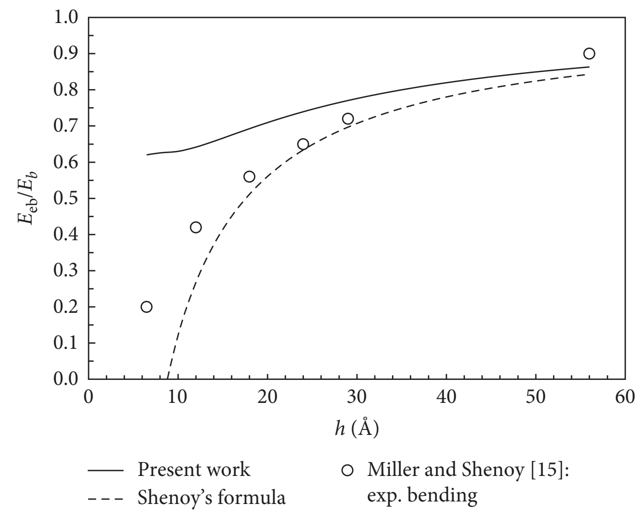

FIGURE 3: Effective bending elastic modulus of Si nanowires.

where,

$$a_1 = E_b b\left\{\frac{1}{12}h_b^3 + \frac{e^m - 1}{2m}h_s h_b^2 + \frac{2[e^m(m-1)+1]}{m^2}h_s^2 h_b + \frac{2[e^m(m^2-2m+2)-2]}{m^3}h_s^3\right\},$$
$$a_2 = \frac{bh_s}{\lambda+1}(\tau_u - \tau_l)\left(\frac{h_b}{2} + \frac{\lambda+1}{\lambda+2}h_s\right). \quad (16)$$

Equation (15) can be used to study the bending deformation of NWs. If the boundary condition of the loaded NW is given, the bending moment can be calculated easily. The bending curvature is expressed by substituting the moment into Equation (15). Then, the height of the neutral axis is expressed by substituting the curvature into Equation (14). The rotation and deflection of NW can be determined after directly integrating Equation (15) once and twice. The flexural rigidity of NW is defined as dM/dw'' on the basis of the bending load. From Equation (15), the normalized effective elastic modulus is obtained as $E_{eb} = a_1/E_b I$:

$$\frac{E_{eb}}{E_b} = \left(1 - \frac{2h_s}{h}\right)^3 + \frac{6(e^m-1)h_s}{mh}\left(1 - \frac{2h_s}{h}\right)^2 + \frac{24[e^m(m-1)+1]h_s^2}{m^2h^2}\left(1 - \frac{2h_s}{h}\right) + \frac{24[e^m(m^2-2m+2)-2]h_s^3}{m^3h^3}. \quad (17)$$

As described in this section, we extend the laminated beam model to the prediction of the size dependence of the effective modulus of NWs. The predictions expressed by Equations (5) and (17) are tested against those by other formulas. The influence of surface elasticity on the size effect of NWs is presented in the following section.

3. Results and Discussion

We first make a comparison with Shenoy's formula to verify our model's prediction. Miller and Shenoy [15] considered surface tension to be contributed by tensile stiffness and flexural rigidity. They obtained the effective modulus of square Si NW: $h = 4.396$ nm, $E_{et} = 0.9E_b$; $h = 8.096$ nm, $E_{eb} = 0.9E_b$. On the basis of these results, we estimated the best-fitting thickness of the surface h_s to be ~0.385 nm and parameter m to be approximately −2. The theoretical prediction for the normalized effective elastic modulus E_{et}/E_b as a function of NW thickness h under tension is displayed in Figure 2, which shows that the prediction of the laminated beam model is in good agreement with that of Shenoy's formula. Figure 3 provides the theoretical estimations of the effective bending elastic modulus E_{eb}/E_b as a function of the NW thickness h. Figure 3 shows that Shenoy's formula underestimates the bending modulus of NWs because it fails to consider the flexural resistance of the surface. Additionally, Shenoy's model cannot predict the bending modulus of NWs with widths of less than 6.5 Å because the defined thickness of the surface layer is negative, and the effective bending modulus E_{eb} is also negative if $h < 8h_s$. The softening effect of the surface on the NWs can easily be represented by the laminated beam model in which one only needs to let $m < 0$ in Equation (17). Moreover, Equations (5) and (17) can predict the tensile and bending moduli of a NW even if it has a small width, and the predicted h_s, E_{et}, and E_{eb} are constantly positive. As found in Equation (17) and Figure 3, the flexural resistance of the surface is naturally considered in the model and the predicted effective bending modulus E_{eb} is slightly higher than the experimental value. Notably, the thickness of the surface layer (h_s) has a greater influence on the size dependence of NWs than the surface constant (m).

We compare our model with Chhapadia's formula to further verify its validity. As reported in the previous section, the NW is modeled as a laminated beam, and three parameters are introduced to describe surface elasticity. The size-dependent flexural properties of NWs and the influence of

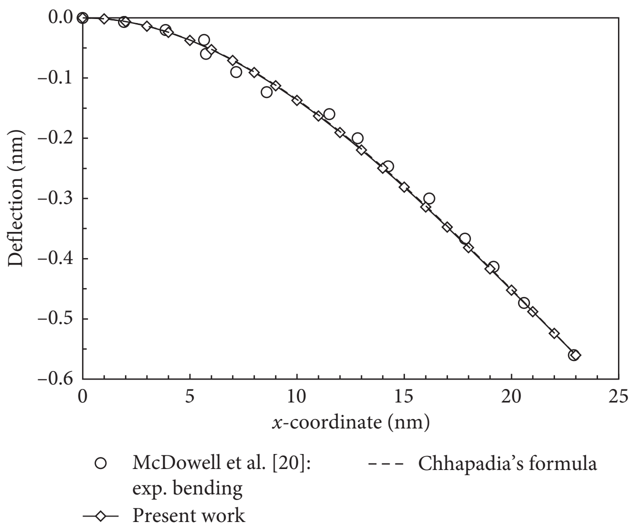

Figure 4: Plot of deflection vs. axial distance.

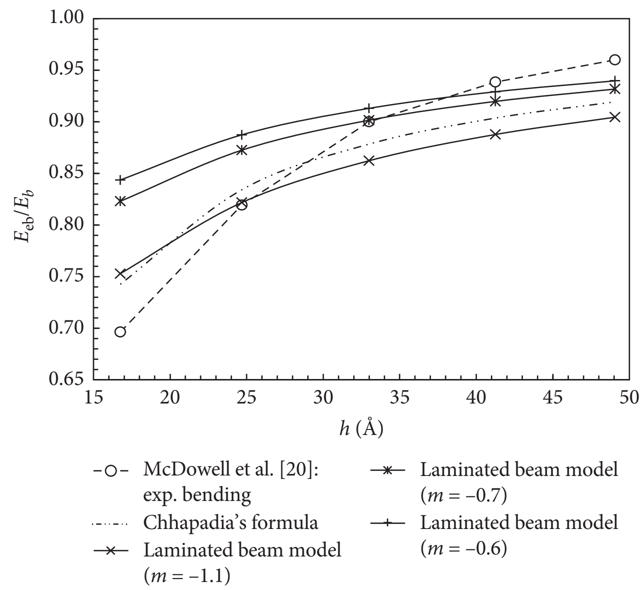

Figure 5: Effective bending elastic modulus of Ag nanowires ($m < 0$).

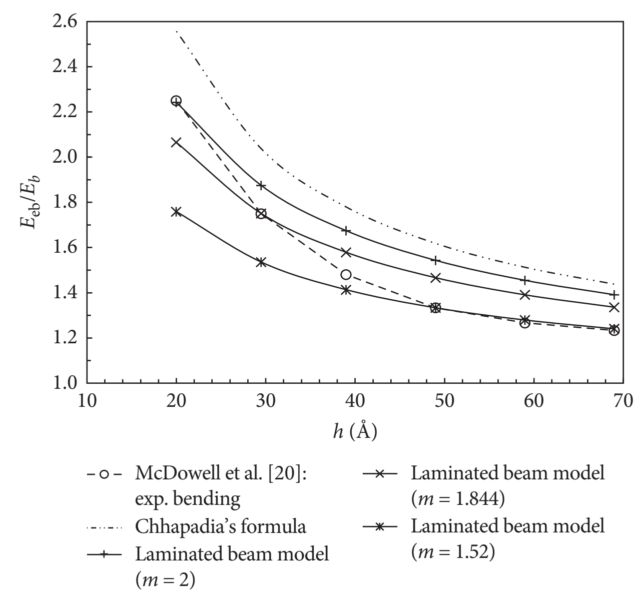

Figure 6: Effective bending elastic modulus of Ag nanowires ($m > 0$).

material parameters on the bending deformation of NWs are discussed here. Chhapadia et al. [19] and McDowell et al. [20] performed atomistic simulations of silver NWs with thicknesses ranging from 1.6 to 6 nm. In their works, they used the Gurtin–Murdoch and Steigmann–Ogden models to determine curvature-dependent surface elasticity and applied two configurations ($\langle 110 \rangle$ and $\langle 100 \rangle$ axially oriented NWs) to fit the simulation to the theoretical models. For a cantilever beam, load F along the y-direction is applied at $x = l$, and the bending moment is $F(x - l)$. The deflection δ at $x = l$ can also be measured by the laminated beam model. By considering the boundary condition at the fixed end and substituting δ into F, we can express deflection as $w = \delta x^2(x - 3l)/2l^3 + a_2 x^2 (x - l)/4a_1 l$. By letting $l = 23$ nm, $h_u = h_l = 0.21158$ nm, $h_b = 6.47684$ nm, $E_b = 70$ GPa, $b = 2.25$ nm, $m = 1.52$, $\lambda = 0.1$, $\tau_u - \tau_l = 60$ Mpa, and $\delta = 0.56$ nm, we predict the bending of silver NWs. Deflection vs. position is shown in Figure 4. The deflections predicted by atomistic simulation, Chhapadia's model, and the laminated beam model follow a cubic polynomial relation with the x-coordinate.

Figure 5 shows the four model predictions for the softening effect on the $\langle 100 \rangle$ axially oriented silver NW. We observe that the model results are in good agreement with direct atomistic simulations [19]. Chhapadia's formula underestimates the bending modulus of the NW with high thickness, i.e., $h \geq 32.5$ nm, likely due to the thickness of the surface layer. In Chhapadia's formula, the bending energy is overestimated, and the thickness is defined as the ratio of energy stored under bending to that under stretching. The laminated beam model provides a better prediction of $h_s \approx 0.21$ nm than Chhapadia's definition ($h_s \approx 0.673$ nm). Our prediction for the surface thickness of the NW is between the two estimations of Shenoy's formula and Chhapadia's model. Figure 5 shows that the effective bending modulus of NW E_{eb} increases with the surface elastic constant m. We can then conclude that with the increase in m, the change in the elasticity in the transition from the bulk region to the external surface layer increases, whereas the influence of the surface layer diminishes.

Figure 6 shows the four model predictions for the stiffening effect on the $\langle 110 \rangle$ axially oriented silver NW. Chhapadia's formula overestimates the bending modulus of the NW with positive surface constants because it overestimates surface thickness. In summary, an increase in characteristic length results in a decline in size dependence. Shenoy's formula, Chhapadia's formula, and the laminated beam model can provide a good prediction of the effective modulus when the characteristic length of NW is large. However, evident differences are observed between the predictions of the continuum

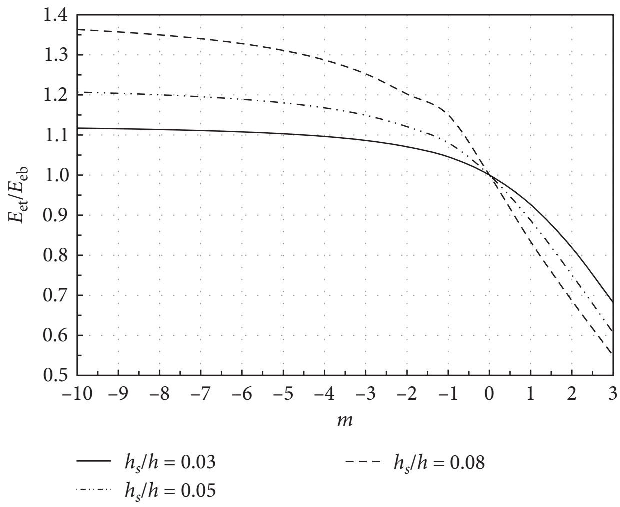

FIGURE 7: Prediction for stiffening effect and softening effect.

mechanics models mentioned in this paper and the experimental results when the characteristic length of NW is small. The reader is encouraged to refer to a new explanation regarding the quantum effect [24] and surface energy density [25] of nanostructures.

Figure 7 shows the ratio of tensile modulus to bending modulus E_{et}/E_{eb} as a function of surface constant m with several different surface thicknesses; $E_{et}/E_{eb} > 1$ when $m < 1$, and $E_{et}/E_{eb} < 1$ when $m > 1$. The transformation of the ratio from a negative to a positive surface constant (m) well reflects the stiffening and softening effects of the NW. A high surface elasticity increases the bending modulus more than the tensile modulus. A low surface elasticity decreases the bending modulus more than the tensile modulus. Notably, surface thickness amplifies the stiffening and softening effects. A thick surface increases the tensile modulus when $m < 1$ and increases the bending modulus when $m > 1$. The laminated beam model could well predict the size-dependent surface effect of NWs in accordance with Shenoy's formula and Chhapadia's model.

4. Conclusion

In this work, a laminated beam model is employed to investigate the size dependency of NWs. The surface is treated as a material layer with definite thickness abutting the core bulk and constraining the deformation of NW. The results that we presented in the last section clearly show that the predictions of the laminated beam model are in good agreement with the experimental results. The laminated beam model has two advantages over other continuum mechanics models: first, it provides a clear definition of surface thickness, which is the thickness of the domain wherein elasticity changes from the bulk region to the external surface. In contrast to the indirect definition of surface thickness as the ratio of the surface constant to the bulk modulus, surface thickness is a real constant in the laminated beam model. The geometric interpretation of surface thickness is evident and constantly positive. In fact, the two surface constants h_s and m in our model are new representations of surface elasticity. Second, the surface elastic constant m can be positive or negative. Hence, we can easily use the laminated beam model to explain the stiffening effect ($m > 0$) and softening effect ($m < 0$) of NW. Owing to the definite surface thickness, the surface layer naturally has tensile stiffness and flexural rigidity. The constants h_s and m are directly employed to describe the surface effect of NWs. In general, surface thickness has a great influence on the effective modulus of NWs. As a consequence, determining surface thickness and describing surface elasticity remain two important problems of investigations on size dependency. Given that NWs are considered as nanolaminated composite materials, the laminated beam model can be easily extended to analyze their size-dependent mechanical properties.

Data Availability

The cited data about surface elastic constants of silver nanowire used to support the findings of this study are included within the referenced article. The data have been used to verify our theoretical prediction.

Conflicts of Interest

The authors declare that they have no conflicts of interest.

Acknowledgments

The authors gratefully acknowledge the financial supports to this work from the National Engineering Laboratory for Highway Tunnel Construction Technology (grant no. NELFHT201702), the Chunhui Project of Ministry of Education of the People's Republic of China (grant no. z2014040), Natural Science Foundation of Sichuan (grant no. 2022NSFSC0443), Research Project of Sichuan Provincial Department of Education (grant no. 15ZA0138), and Key Research Project of Xihua University (grant no. z1320608).

References

[1] D. Appell, "Nanotechnology: wired for success," *Nature*, vol. 419, pp. 553–555, 2002.

[2] E. Gil-Santos, D. Ramos, J. Martínez et al., "Nanomechanical mass sensing and stiffness spectrometry based on two-dimensional vibrations of resonant nanowires," *Nature Nanotechnology*, vol. 5, pp. 641–645, 2010.

[3] S. Ding, Y. Tian, Z. Jiang, and X. He, "Molecular dynamics simulation of joining process of Ag–Au nanowires and mechanical properties of the hybrid nanojoint," *AIP Advances*, vol. 5, no. 5, Article ID 057120, 2015.

[4] S. Wang, Z. Shan, and H. Huang, "The mechanical properties of nanowires," *Advanced Science*, vol. 4, no. 4, Article ID 1600332, 2017.

[5] M. Friák, M. Šob, and V. Vitek, "*Ab initio* study of the ideal tensile strength and mechanical stability of transition-metal disilicides," *Physical Review B*, vol. 68, no. 18, Article ID 184101, 2003.

[6] W. Zhang, T. Wang, and X. Chen, "Effect of surface stress on the asymmetric yield strength of nanowires," *Journal of Applied Physics*, vol. 103, no. 12, Article ID 123527, 2008.

[7] P. Gupta and A. Kumar, "Effect of surface elasticity on extensional and torsional stiffnesses of isotropic circular nanorods," *Mathematics and Mechanics of Solids*, vol. 24, no. 6, pp. 1613–1629, 2019.

[8] M. E. Gurtin and A. Ian Murdoch, "Surface stress in solids," *International Journal of Solids and Structures*, vol. 14, no. 6, pp. 431–440, 1978.

[9] H. L. Duan, J. Wang, Z. P. Huang, and B. L. Karihaloo, "Size-dependent effective elastic constants of solids containing nano-inhomogeneities with interface stress," *Journal of the Mechanics and Physics of Solids*, vol. 53, no. 7, pp. 1574–1596, 2005.

[10] A. C. Eringen and D. G. B. Edelen, "On nonlocal elasticity," *International Journal of Engineering Science*, vol. 10, no. 3, pp. 233–248, 1972.

[11] S. Hosseini-Hashemi, I. Nahas, M. Fakher, and R. Nazemnezhad, "Surface effects on free vibration of piezoelectric functionally graded nanobeams using nonlocal elasticity," *Acta Mechanica*, vol. 225, pp. 1555–1564, 2014.

[12] R. A. Arpanahi, S. Hosseini-Hashemi, S. Rahmanian, S. H. Hashemi, and A. Ahmadi-Savadkoohi, "Nonlocal surface energy effect on free vibration behavior of nanoplates submerged in incompressible fluid," *Thin-Walled Structures*, vol. 143, Article ID 106212, 2019.

[13] Z.-Q. Wang, Y.-P. Zhao, and Z.-P. Huang, "The effects of surface tension on the elastic properties of nano structures," *International Journal of Engineering Science*, vol. 48, no. 2, pp. 140–150, 2010.

[14] Y. Yao and C. Shaohua, "Surface effect in the bending of nanowires," *Mechanics of Materials*, vol. 100, pp. 12–21, 2016.

[15] R. E. Miller and V. B. Shenoy, "Size-dependent elastic properties of nanosized structural elements," *Nanotechnology*, vol. 11, no. 3, pp. 139–147, 2000.

[16] M. H. Korayem and M. Zakeri, "Dynamic modeling of manipulation of micro/nanoparticles on rough surfaces," *Applied Surface Science*, vol. 257, no. 15, pp. 6503–6513, 2011.

[17] M. Ahmadi, R. Ansari, and M. Darvizeh, "Free and forced vibrations of atomic force microscope piezoelectric cantilevers considering tip-sample nonlinear interactions," *Thin-Walled Structures*, vol. 145, Article ID 106382, 2019.

[18] D. J. Steigmann and R. W. Ogden, "Elastic surface–substrate interactions," *Proceedings of the Royal Society of London. Series A: Mathematical, Physical and Engineering Sciences*, vol. 455, no. 1982, pp. 437–474, 1999.

[19] P. Chhapadia, P. Mohammadi, and P. Sharma, "Curvature-dependence surface energy and implications for nanostructures," *Journal of the Mechanics and Physics of Solids*, vol. 59, no. 10, pp. 2103–2115, 2011.

[20] M. T. McDowell, A. M. Leach, and K. Gaill, "Bending and tensile deformation of metallic nanowires," *Modelling and Simulation in Materials Science and Engineering*, vol. 16, no. 4, Article ID 045003, 2008.

[21] C. Q. Chen, Y. Shi, Y. S. Zhang, J. Zhu, and Y. J. Yan, "Size dependence of Young's modulus in ZnO nanowires," *Physical Review Letters*, vol. 96, no. 7, Article ID 075505, 2006.

[22] H. Yao, G. Yun, N. Bai, and J. Li, "Surface elasticity effect on the size-dependent elastic property of nanowires," *Journal of Applied Physics*, vol. 111, no. 8, Article ID 083506, 2012.

[23] S. Hosseini-Hashemi and R. Nazemnezhad, "An analytical study on the nonlinear free vibration of functionally graded nanobeams incorporating surface effects," *Composites Part B: Engineering*, vol. 52, pp. 199–206, 2013.

[24] Y. Zhu, Y. Wei, and X. Guo, "Gurtin–Murdoch surface elasticity theory revisit: an orbital-free density functional theory perspective," *Journal of the Mechanics and Physics of Solids*, vol. 109, pp. 178–197, 2017.

[25] Y. Yao, S. Chen, and D. Fang, "An interface energy density-based theory considering the coherent interface effect in nanomaterials," *Journal of the Mechanics and Physics of Solids*, vol. 99, pp. 321–337, 2017.